Desalination and Water Treatment
www.deswater.com

doi: 10.5004/dwt.2018.22611

122 (2018) 42–49
August

Synthesis, characterization of ZVI nanoparticles and its application for the removal of phenol from wastewater

R. Sridar[a,*], U. Uma Ramanane[b], M. Rajasimman[c]

[a]*Department of Chemical Engineering, Pondicherry Engineering College, Puducherry, India, email: sivakamisridar9@pec.edu (R. Sridar)*
[b]*Department of Civil Engineering, Pondicherry Engineering College, Puducherry, India*
[c]*Department of Chemical Engineering, Annamalai University, Annamalai Nagar, Chidambaram, Tamil nadu 608002, India*

Received 7 March 2018; Accepted 9 June 2018

ABSTRACT

This study aims at the synthesis of zero valent iron (ZVI) nanoparticles and its application for the removal of phenol by adsorption. The ZVI nanoparticles were synthesized using borohydride reduction method. The structural, morphological properties of synthesized ZVI nanoparticles were thoroughly investigated by X-ray diffraction, scanning electron microscopy and particle size distribution. The effect of initial pH, contact time, initial concentration of phenol and nano ZVI dosage on phenol removal has been studied. From the results, the optimum conditions for the maximum removal of phenol at 100 ppm were found to be: pH – 3, contact time – 30 min, sorbent dosage – 0.5 g/L. Isotherm and kinetic studies were performed from the data obtained from adsorption studies. From the results, it was observed that the Freundlich isotherm ($R^2 = 0.9836$) fits the sorption data well when compared with other isotherm. From the kinetic studies, it was inferred that the sorption process follows pseudo-first order ($R^2 = 0.9836$) adsorption kinetics. This study also compares the performance of synthesized nanoparticles for the removal of phenol from industrial and synthetic wastewater.

Keywords: Phenol; Nanoparticles; Synthesis; Kinetics; Isotherm; Sorption

1. Introduction

In the earth's crust, the fourth largest liberal element is iron. Zero valent iron (ZVI) nanoparticles are the first generation nanoparticles of interest to environmental remediation. ZVI is a strong reducing agent with higher reactivity. The reaction rates for nano zero-valent iron (nZVI) were much faster and also the sorption capacity is much higher compared with normal granular iron. Removal of contaminants occurs on the surface of ZVI nanoparticles. ZVI nanoparticles are extremely effective for the removal of a wide range of common environmental pollutants such as pharmaceutical products, chlorinated organic solvents, phenolic compounds, pesticides, nitrates, chromium, malathion, aromatic compounds, arsenic and polychlorinated biphenyls [1–8]. The removal of pollutants by the use of these nanoparticles occurs in a short time when compared with a conventional process such as biodegradation.

ZVI as a remediation technology has the following advantages such as that it is relatively inexpensive, non-toxic, highly energy efficient and mainly used technique for treating contaminated groundwater in-situ by utilizing passive reactive barriers. There are many processes available for synthesis of ZVI nanoparticles under physical, chemical and biological methods [9–18]. The major difference between all the above methods is that the toxicity is less in physical and biological methods. But the irregular shape, time consumption and lesser yield are the major disadvantages [9]. In chemical method, synthesis of nZVI can be largely obtained by borohydride reduction method. Reduction method is

---

* Corresponding author.

Presented at the 3rd International Conference on Recent Advancements in Chemical, Environmental and Energy Engineering, 15–16 February, Chennai, India, 2018.

1944-3994/1944-3986

used as it is cheap and simple. It is normally done in all chemical laboratories with simple chemical reagents and does not need any sophisticated instruments.

Industrial use of phenol and its derivatives over the past decades have led to severe environmental pollution. Due to the harmful nature of phenols and their potential hazardous effects on human health, they have been classified as toxic pollutants. Since phenol is harmful to organisms even at low concentration and is difficult to be degraded biologically, it has been classified as a priority pollutant in wastewater. There are many physical, chemical and biological treatment methods available for the removal of phenol but all these methods have associated problems such as secondary effluent, hazardous and harmful end products, high energy consumption, long reaction times, uneconomical and low efficiency [19,20]. These problems can be overcome by the use of nanotechnology which is simple when compared with other methods and complete removal of the pollutants is possible [21]. In this study, nZVI is synthesized and it is utilized for the removal of phenol from synthetic and industrial wastewater.

2. Materials and methodology

2.1. Synthesis of zero valent iron nanoparticles

Synthesis of nanoscale iron particles with the sodium borohydride method was used. The major advantages of this chemical reduction method are its simplicity and chemical homogeneity and thus it can be carried out in almost any laboratory without any special equipment. Moreover, the particles prepared by this method have an amorphous structure, which lends them higher reactivity when used as chemical catalysts.

$$4Fe^{3+} + 3BH^{-}_{4} + 9H_2O \rightarrow 4Fe^{0}\downarrow + 3H_2BO^{-}_{3} + 12H^{+} + 6H_2 \qquad (1)$$

Ferrous sulphate heptahydrate ($FeSO_4.7H_2O$) is reduced to iron (Fe) using sodium borohydride as reducing agent in the presence of ethanol to avoid oxidation of iron to iron oxide. The synthesis of iron nanoparticles was carried out in a flask reactor with three open necks (Fig. 1). The central neck was housed with a tunable mechanical stirrer. Ethanol was added to preserve the nano iron particles from oxidation.

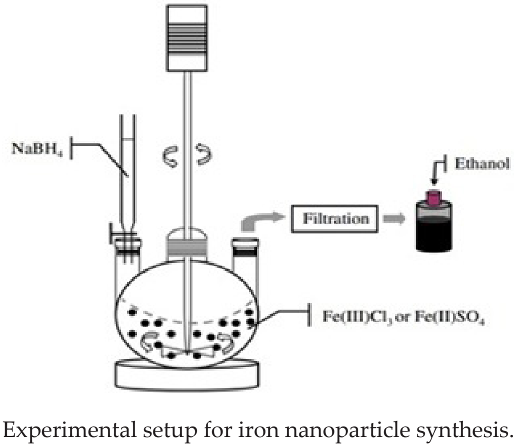

Fig. 1. Experimental setup for iron nanoparticle synthesis.

5 g of $FeSO_4.7H_2O$ was dissolved in 35 mL distilled water and 15 mL ethanol was taken in a conical flask and the solution was stirred well. 1 g of $NaBH_4$ was dissolved in 50 mL of distilled water and taken in another conical flask. For better growth of iron nanoparticles, excess borohydride is required. The borohydride solution was poured in a burette and added drop by drop into ferrous sulphate solution with vigorous stirring. After the addition of first drop of sodium borohydride solution, appearance of black solid particles was observed and then the remaining sodium borohydride solution was added completely to accelerate the reduction reaction. The mixture was thoroughly stirred for 30 min after the complete addition of borohydride solution. The filtration technique was used to separate the black iron nanoparticles from the liquid phase. Two sheets of Whatman filter paper were used for filtration. The solid particles were washed three times using 40 mL of absolute ethanol to completely remove the water present in the solution. This washing process was the key step of synthesis since it prevents the rapid oxidation of ZVI nanoparticles. For storage, a thin layer of ethanol was added to preserve the nano iron particles from oxidation.

2.2. Preparation of synthetic effluent and industrial phenolic wastewater

Stock phenol solution was prepared by dissolving 1.0 g of phenol in freshly boiled and cooled distilled water and diluted to 1 L (1 mL = 1 mg phenol). Working solution A: dilute 10 mL stock phenol solution to 1 L with distilled water (1 mL = 10 µg phenol). Working solution B: dilute 100 mL of working solution A to 1,000 mL with distilled water (1 mL = 1 µg phenol). The concentration of phenol in the synthetic effluent was analytically determined by 4-aminoantipyrine method [22].

The conditions of phenol removal were essentially the same as for assay with the synthetic wastewater, except the phenol solution was replaced by industrial wastewater obtained from Yaaco Pharma Private Limited, Mettupalayam, Pondicherry. The sample was stored at 4°C and utilized for the batch experiments within 3 d. The characteristics of industrial wastewater were analyzed and it is given in Table 1. 500 mL of the sample is measured in a beaker and then transferred to the distillation apparatus. For most samples, a preliminary distillation is required to remove interfering materials.

2.3. Removal of phenol using zero valent iron nanoparticles

The effect of initial pH, initial concentration of phenol, contact time and nZVI dosage was studied. Samples of different pH (3, 4, 5, 6 and 7), different initial concentrations of phenol (100, 200, 300 and 400 ppm) were prepared. The samples were

Table 1
Characteristics of wastewater from pharmaceutical industry

Parameter	Range or average
pH	6.1 – 7
BOD_5, mg/L	480–590
COD (mg/L), mg/L	1,100–1,200
Phenol (mg/L), ppm	45–58
Turbidity (NTU)	7

treated with nZVI of different dosage for different intervals of contact time such as 10, 20, 30 and 40 min. The experiments were conducted in a batch reactor with 500 mL of diluted phenol solution (100 ppm) which has a pH of 6 (natural pH), 0.25 g of ZVI was added to initiate the process. The solution was stirred well using magnetic stirrer and the sample was taken for every 10 min and was filtered to remove ZVI nanoparticles.

The filtered sample was analytically measured by 4-aminoantipyrine method [22]. The sample solution was analyzed in UV spectrophotometer at a wavelength of 510 nm with an optical path length of 1 cm and the absorbance value was obtained. Again, phenol solution of 100 ppm initial concentration was prepared and the above procedure was repeated for different pH, different dosage of nZVI and different contact time. The same methodology was adopted for industrial effluent. For industrial effluent, the sample was initially distilled and the distillate should be used for further purpose. From the standardization of phenol, to get the relationship between concentration and absorbance, a calibration chart was prepared. The calibration curve was prepared by varying the amount of phenol in the range of 2–500 ppm.

The amount of phenol adsorbed per unit mass of adsorbent (q_e, mg/g):

$$q_e = \frac{\left(C_0 - C_e\right)V}{m} \tag{2}$$

The amount of adsorbed phenol per unit mass of adsorbent at time t (q_t, mg/g):

$$q_t = \frac{\left(C_0 - C_t\right)V}{m} \tag{3}$$

where V is the volume of the solution treated in L, C_0 is the initial concentration of the phenol in mg/L, C_e is the equilibrium phenol concentration in mg/L, C_t (mg/L) is the concentration of adsorbent at time t and m is the mass of adsorbent in g.

2.4. Characterization studies

2.4.1. X-ray diffraction analysis

X-ray diffraction (XRD) is an analytical technique which is used for phase identification of a crystalline material. It can provide information about the unit cell dimensions of natural and synthesized compounds. Iron nanoparticles were placed in a glass holder and scanned from 40° to 80°. This scan range covered all major species of iron and iron oxides. The ZVI characteristic peaks of the sample are detected at 44.7°, which confirms the presence of ZVI nanoparticles in the sample (Fig. 2). The grain size calculated using Scherrer's formula for ZVI nanoparticles.

$$D = \frac{0.9\lambda}{B\cos\theta}$$

$$D = \frac{0.9 \times 1.54 \times 10^{-10}}{0.00514 \times \cos\left(11.99\right)} \tag{4}$$

$$D = 28.11 \text{ nm}$$

2.4.2. Scanning electron microscopy

Scanning electron microscopy (SEM) is used as a tool to obtain the image of a surface. The nZVI were filtered from the ethanol solution and vacuum dried carefully. The dried samples were then sputter-coated with gold for SEM analysis. The resulting ZVI nanoparticles were composed of spherical rod shape particles (Fig. 3). These structures were used to increase the available surface area for reaction.

2.4.3. Particle size distribution analysis of zero valent iron nanoparticles

Size distribution was determined with a Malvern Zeta Sizer Nano S (Malvern Instruments Ltd., UK) by the dynamic light scattering technique. The specifications are given in Table 2. The characterization of synthesized ZVI nanoparticles was done by particle size distribution (PSD) method based on laser diffraction technique. Refractive index for ZVI nanoparticles is 2.87.

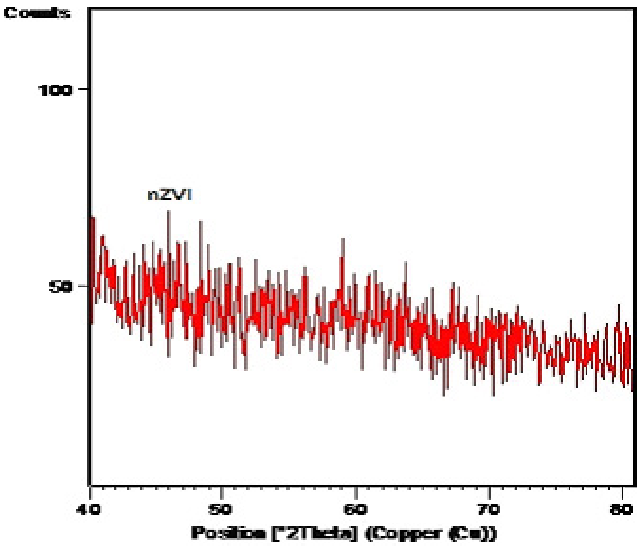

Fig. 2. XRD image of zero valent iron nanoparticles.

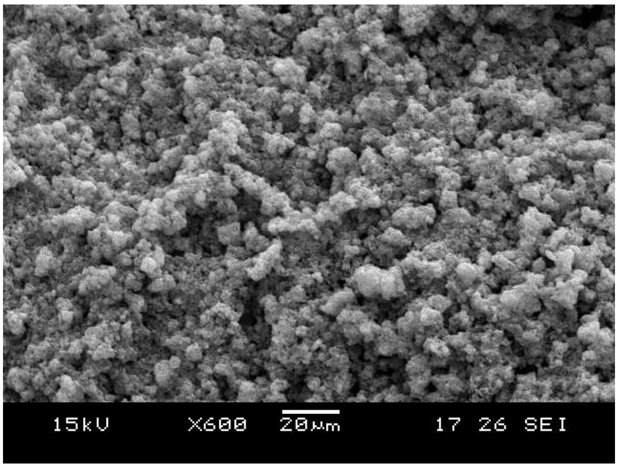

Fig. 3. SEM image of zero valent iron nanoparticles at 20 μm/600X.

Table 2
Specification of particle size analyzer

Specification	Units
Measurement	0.3 nm–10.0 microns (diameter)
Measurement principle	Dynamic light scattering
Minimum sample volume	12 µL
Accuracy	Better than ±2% on NIST traceable latex standards
Precision/repeatability	Better than ±2% on NIST traceable latex standards
Sensitivity	0.1 mg/mL

From the PSD chart (Fig. 4), the mean diameter of iron nanoparticles was found to be 68.92 nm. The PSD results also show that most of the particles have a size ranging between 30 and 100 nm.

2.4.4. Isotherm and kinetic study

In this study, the batch experimental data were fitted with the following isotherms namely Langmuir and Freundlich to study the applicability of the isotherms. Also the kinetic models namely, Lagergren's [38] pseudo-first order model, Ho and McKay's [39] pseudo-second order model are employed in this study. The kinetic model parameters are determined using MATLAB software.

3. Results and discussion

3.1. Effect of contact time and pH

The effect of contact time on the removal of phenol from aqueous solutions at a pH of 3, 4, 5, 6 and 7 is shown in Fig. 5. The results obtained from contact time studies show that the removal of phenol increases with increase in contact time. The sorption of phenol onto nZVI was rapid for first 20 min and equilibrium was nearly reached after 30 min irrespective of initial pH of the solution. A further increase in the contact time has a negligible effect on the removal of phenol by the nanoparticles. The removal efficiency of phenol was higher in the beginning due to a larger surface area of the nZVI being available for phenol removal.

The pH of the solution is one of the most critical parameters in the removal of phenol from aqueous solutions. This parameter is directly related to the competing ability of hydrogen ions with phenol to active sites on the nZVI. The effect of solution pH on the sorption of phenol onto nZVI nanoparticles was evaluated within the pH range of 3.0–7.0 and the result is shown in Fig. 5. The increase in initial pH affected the phenol removal negatively and pH of 3 was found to be the optimum for nZVI. Phenol removal recorded its maximum removal efficiency of 91.8% at a pH of 3 in 30 min.

3.2. Effect of initial dosage

The effect of variations in nZVI dosage on the sorption of phenol is shown in Fig. 6. The nZVI dosage is an important parameter because this estimates the sorption capacity for a given initial phenol concentration. During the process, initial phenol concentration and pH were maintained at 100 ppm and 3, respectively. The increase in nZVI dosage from 0.3 to 1.0 g/L accelerated the removal of phenol moderately, which is mainly due to the increase in number of active sites. The removal of phenol was increased when nZVI dosage was increased up to 0.5 g/L and further increase in nanoparticles dosage did not enhance the sorption to a great extent. The maximum removal efficiency of phenol onto nZVI was found to be 91.8% at nZVI of 0.5 g/L and 93.4% at 1.0 g/L of sorbent dosage.

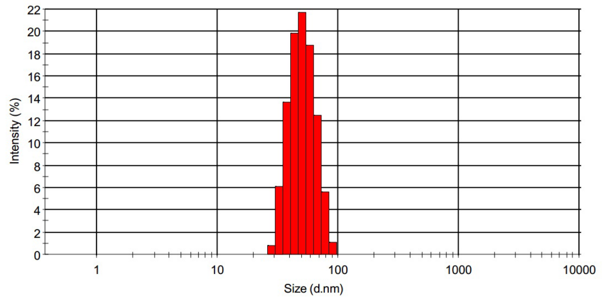

Fig. 4. Particle size distribution of zero valent iron nanoparticles.

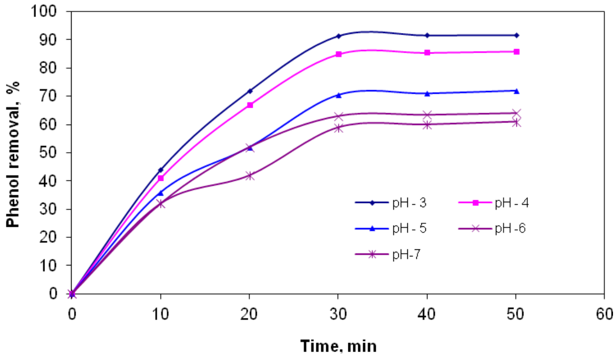

Fig. 5. Effect of solution pH (experimental conditions: phenol concentration = 100 ppm, nZVI dosage = 0.5 g/L).

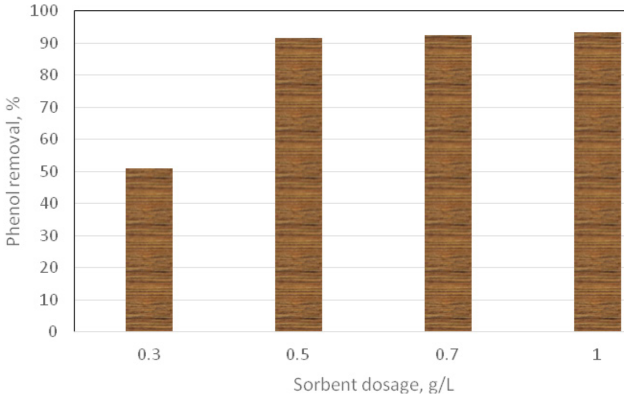

Fig. 6. Effect of nZVI dosage (experimental conditions: phenol concentration = 100 ppm, solution pH = 3 and contact time = 30 min).

3.3. Effect of initial concentration of phenol

The effect of initial concentration of phenol on the sorption of phenol by nZVI is shown in Fig. 7. The results showed that the reaction time for the sorption of phenol extended with an increase in initial concentration of phenol from 100 to 400 mg/L. This is due to the fact that at higher concentrations, phenol molecules may get adsorbed on the surface of nZVI occupying a large number of active sites. The removal efficiency of phenol was found to decrease with an increase in initial concentration of phenol.

3.4. Phenol removal from industrial effluent

The phenol concentration in the industrial effluent was found to be much lower when compared with the synthetic wastewater prepared in the laboratory. The removal efficiency was also found to be low when compared with the synthetic wastewater. The reason for the poor efficiency of removal may be due to high viscosity and interference of other particles in industrial wastewater. The removal of phenol from industrial samples at a pH of 6 for nZVI is shown in Fig. 8. The sorption of phenol onto nZVI was found to be relatively less when compared with synthetic effluent. The efficiency for ZVI nanoparticles is 82%. From the above results, ZVI nanoparticles were found to be good and efficient with respect to removal of phenol. With respect to cost, it takes 12 rupees for removal of 1 L solution of phenol for ZVI nanoparticles.

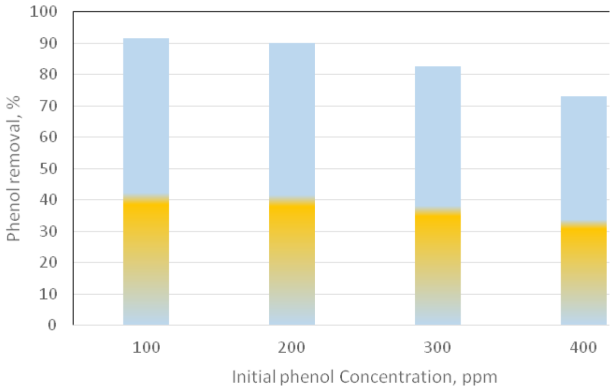

Fig. 7. Effect of different initial concentration (experimental conditions: nZVI dosage = 0.5 g, pH = 3, contact time = 30 min).

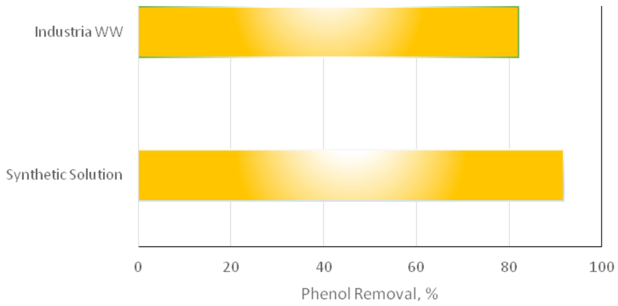

Fig. 8. Phenol removal from industrial effluent (experimental conditions: pH = 6, dosage of nZVI = 0.5 g/L).

4. Isotherm study

4.1. Langmuir isotherm

Langmuir [23] anticipated a theory to clarify the sorption of gas molecules onto metal surfaces. It has been successfully applied to many other monolayer sorption processes. Langmuir's model of sorption depends on the hypothesis that intermolecular forces decrease rapidly with distance and thus forecast the existence of monolayer coverage of the sorbate in the outer surface of the sorbent. Hypothetically, the sorbent has a definite capacity for the sorbate. Thus, a saturation value is attained after which no further sorption can take place. The linear form of Langmuir isotherm is given by:

$$\frac{1}{q_e} = \frac{1}{q_m b C_e} + \frac{1}{q_m} \tag{5}$$

where q_m is the monolayer sorption capacity of the sorbent (mg/g), q_e is the equilibrium phenol uptake by the sorbent (mg/g), C_e is the equilibrium phenol concentration in the solution (mg/L) and b is the Langmuir sorption constant (L/mg) related to the free energy of sorption. The equilibrium uptake (q_e) is estimated from the experimental data using Langmuir isotherm. The constants were evaluated from the Langmuir isotherm plot (Fig. S1) and are given in Table 3. The maximum sorption capacity of ZVI nanoparticles was found to be 47.61 mg/g. A comparison has been made for the sorption capacity of various sorbents and it is presented in Table 4. From Table 4, it is inferred that the sorption capacity of ZVI nanoparticles is superior to most of the sorbent and comparable with others.

4.2. Freundlich isotherm

The Freundlich [24] isotherm is an empirical equation used to describe heterogeneous systems; it is characterized by the heterogeneity factor 1/*n*. The linear form of Freundlich isotherm is represented by the equation

$$\log q_e = \log K_f + \frac{1}{n}\log C_e \tag{6}$$

where C_e is the equilibrium concentration (mg/L), q_e is the amount of phenol adsorbed at equilibrium (mg/g), $\frac{1}{n}$ is the empirical parameter relating the sorption intensity and K_f is the constant relating the sorption capacity, which varies with the heterogeneity of the material. The constants were

Table 3
Langmuir, Freundlich constants for the sorption of nZVI nanoparticles

Isotherm model	Parameters	Values
Langmuir	q_{max}	47.61 mg/g
	b	0.2442
	R^2	0.981
Freundlich	K_f	31.04
	$1/n$	0.077
	R^2	0.9836

Table 4
Comparison of uptake of phenol using various sorbents

Sorbent	Capacity, mg/g	Reference
CNTs	15.9	[25]
Synthetic resin MCM – 41	11.4	[26]
PHEMA microbead modified sorbent	8 to 16.1	[27,28]
Samla coal	13.3	[29]
Red mud	59.2	[30]
Bagasse fly ash	23.83	[31]
Carbonaceous sorbent	17.2	[32]
Blast furnace sludge	7.5	
Blast furnace dust	5.3	
Activated sewage sludge	42	[33]
GAC	350	[34]
Clay	30.3	[35]
ZnO nano tube	20.408	[36]
Aloe vera	71.73	[37]
Mesquite	54.27	[37]
nZVI nanoparticle	47.61	This study

evaluated and are tabulated in Table 3. The plot is shown in Fig. S2. From Table 3, it is observed that the Freundlich isotherm fits the phenol sorption data well when compared with Langmuir isotherm based on R^2 value.

5. Sorption kinetics

The study of adsorption dynamics describes the solute uptake rate, and this rate controls the habitation time of adsorbate uptake at the solid–solution interface. Chemical kinetics gives information about reaction pathways and times to reach equilibrium. Sorption kinetics showed a large confidence on physical and chemical characteristics of the sorbent material. Different models have been used to investigate the mechanism of sorption. The consistency between experimental and the model outcome values is expressed by the correlation coefficients. High R^2 value indicates that the model fruitfully describes the kinetics of sorption process. When the sorbent is used as a free and small-sized sorbent suspension in a well-agitated batch system, all the sorbent binding sites are readily available for the phenol uptake.

5.1. Pseudo-first order model

Lagergren [38] suggested a pseudo-first order equation for the sorption of a liquid/solid system based on the solid capacity. The linear form of the Lagergren's pseudo-first order rate equation is:

$$\log(q_e - q_t) = \log q_e - \frac{k_1}{2.303}t \tag{7}$$

where k_1 is the rate constant of the equation (min^{-1}), q_t and q_e are the amount of the phenol adsorbed at any time t and at equilibrium (mg/g), respectively.

Table 5
Kinetic model parameters for the sorption of phenol

Sl. no	Kinetic model	Parameters	Values
1	Pseudo-first order	k_1 (min^{-1})	0.1082
		R^2	0.950
2	Pseudo-second order	k_2 ((g/mg)min)	0.001332
		R^2	0.979

5.2. Pseudo-second order model

The pseudo-second order model predicts the sorption behavior over the whole time of adsorption [39].

$$\frac{t}{q_t} = \frac{1}{k_2 q_e^2} + \frac{1}{q_e}t \tag{8}$$

where k_2 is the rate constant of second-order equation (g/mg min), q_t and q_e are the amount of the phenol adsorbed at any time and at equilibrium (mg/g), respectively, and t in minutes. The sorption rate constants, k_1 and k_2, were determined from the graph given in Figs. S3 and S4, respectively. The rate constant values along with R^2 values are given in Table 5. The correlation coefficients show that the pseudo-second order model fits better than the pseudo-first order model for the sorption of phenol.

6. Conclusions

In this work, ZVI nanoparticles were synthesized using borohydride reduction method. The structural, morphological properties of ZVI nanoparticles were thoroughly investigated by XRD, SEM and PSD. The removal of phenol by sorption using ZVI nanoparticles was studied. The effect of initial pH, contact time, initial concentration of phenol and nZVI dosage on phenol removal was studied. The performance of ZVI nanoparticles were also compared based on their efficiency and cost for synthetic and industrial wastewater. A maximum phenol removal efficiency of 91.8% was achieved using the synthesized nZVI particles. This study clearly shows that the ZVI nanoparticles can be effectively applied for the removal of phenol from industrial water.

References

[1] S. Adami, A. Fakhri, Adsorption of 4-chloro-2-nitrophenol by zero valent iron nanoparticles and Pd-doped zero valent iron nanoparticles surfaces: isotherm, kinetic and mechanism modeling, J. Phys. Chem. Biophys., 3 (2013) 115.

[2] C.F. Chen, N.T. Binh, C.W. Chen, C.D. Dong, Removal of polycyclic aromatic hydrocarbons from sediments using sodium persulfate activated by temperature and nanoscale zero-valent iron, J. Air Waste Manage. Assoc., 65 (2015) 375–383.

[3] D. Prabu, R. Parthiban, P. Senthilkumar, Adsorptive separation of phenol from aqueous solution using nano zero valent iron impregnated cashew nut shell, Int. J. Pharm. Bio. Sci., 6 (2015) 129–140.

[4] R.K. Singhal, B. Gangadhar, H. Basu, V. Manisha, G.R. Naidu, R. Reddy, Remediation of malathion contaminated soil using zero valent iron nano-particles, Am. J. Anal. Chem., 3 (2012) 76–82.

[5] Y. Nakatsuji, Z. Salehi, Y. Kawase, Mechanisms for removal of p-nitrophenol from aqueous solution using zero-valent iron, J. Environ. Manage., 152 (2015) 183–191.

[6] C. Uzum, T. Shahwan, A.E. Eroglu, I. Lieberwirth, T.B. Scott, K.R. Hallam, Application of zero-valent iron nanoparticles for the removal of aqueous Co^{2+} ions under various experimental conditions, Chem. Eng. J., 144 (2008) 213–220.

[7] S. Bhattacharya, I. Saha, A. Mukhopadhyay, D. Chattopadhyay, U. Chand Ghosh, D. Chatterjee, Role of nanotechnology in water treatment and purification: potential applications and implications, Int. J. Chem. Sci. Technol., 3 (2013) 59–64.

[8] A. Rodova, J. Filip, Arsenic immobilization by nanoscale zero-valent iron, Ecol. Chem. Eng., S22 (2015) 1291–1298.

[9] S. Li, W. Yan, W.-x. Zhang, Solvent-free production of nanoscale zero-valent iron (nZVI) with precision milling, Green Chem., 11 (2009) 1618–1626.

[10] A. Babuponnusami, K. Muthukumar, Removal of phenol by heterogenous photo electro Fenton like process using nano-zero valent iron, Sep. Purif. Technol., 98 (2012) 130–135.

[11] Y.P. Sun, X.Q. Li, J. Cao, W.X. Zhang, H.P. Wang, Characterization of zero-valent iron nanoparticles, Adv. Colloid Interface Sci., 120 (2006) 47–56.

[12] C.J. Choi, O. Tolochko, B.K. Kim, Preparation of iron nanoparticles by chemical vapor condensation, Mater. Lett., 56 (2002) 289–294.

[13] L.B. Hoch, E.J. Mack, B.W. Hydutsky, J.M. Hershman, J.M. Skluzacek, T.E. Mallouk, Carbothermal synthesis of carbon-supported nano scale zero-valent iron particles for the remediation of hexavalent chromium, Environ. Sci. Technol., 42 (2008) 2600–2605.

[14] E.S. Yusmartini, D. Setiabudidaya, Ridwan, Marsi, Faizal, Synthesis and characterization of zero-valent iron nanoparticles, Adv. Mater. Res., 1112 (2015) 62–65.

[15] S.S. Chen, H.D. Hsu, C.W. Li, A new method to produce nanoscale iron for nitrate removal, J. Nanopart. Res., 6 (2004) 639–647.

[16] G.E. Hoag, J.B. Collins, J.L. Holcomb, J.R. Hoag, M.N. Nadagouda, R.S. Varma, Degradation of bromothymol blue by greener nano-scale zero-valent iron synthesized using tea polyphenols, J. Mater. Chem., 19 (2009) 8671–8677.

[17] M. Pattanayak, P.L. Nayak, Green synthesis and characterization of zero valent iron nanoparticles from the leaf extract of *Azadirachta indica* (Neem), World J. Nano Sci. Technol., 2 (2013) 6–9.

[18] S. Machado, J.G. Pacheco, H.P.A. Nouws, J.T. Albergaria, Characterization of green zero-valent iron nanoparticles produced with tree leaf extracts, Sci. Total Environ., 533 (2015) 76–81.

[19] V. Amudha, J. Rajesh Banu, Ick Tae Yeom, Efficiency of zero valent iron in the modified Fenton process for the reduction of excess sludge and the key role of citric acid through deflocculation, Desal. Wat. Treat., 71 (2017) 271–279.

[20] G. Sokkanathan, V. Godvin Sharmila, S. Kaliappan, J. Rajesh Banu, Ick TaeYeom, R. Uma Rani, Combinative treatment of phenol-rich retting-pond wastewater by a hybrid upflow anaerobic sludge blanket reactor and solar photo-Fenton process, J. Environ. Manage., 206 (2018) 999–1006.

[21] M. Dineshkumar, A. Sivalingam, M. Thirumarimurugan, Removal of phenol using ZnO nanoparticle in three phase fluidization, Int. J. Eng. Res. Technol., 4 (2015) 1111–1116.

[22] USEPA – 1989, Determination of Phenol: Standard Methods for the Examination of Water and Wastewater Procedures, APHA, AWWA and WPCF, USA, 1989.

[23] I. Langmuir, The adsorption of gases on plane surface of glass, mica and platinum, J. Am. Chem. Soc., 40 (1916) 1361–1368.

[24] H.M.F. Freundlich, Over the adsorption in solution, J. Phys. Chem., 57 (1906) 385–470.

[25] Q. Liao, J. Sun, L. Gao, The adsorption of resorcinol from water using multiwalled carbon nanotubes, Colloids Surf., A, 312 (2008) 160–165.

[26] M. Ghiaci, A. Abbaspura, R. Kia, F. Seyedeyn-Azad, Equilibrium isotherm studies for the sorption of benzene, toluene, and phenol onto organo-zeolites and as-synthesized MCM-41, Sep. Purif. Technol., 40 (2004) 217–229.

[27] A. Denizli, G. Ozkan, M. Ucar, Removal of chlorophenols from aquatic systems with dye-affinity microbeads, Sep. Purif. Technol., 24 (2001) 255–262.

[28] A. Denizli, G. Okan, M. Ucar, Dye-affinity microbeads for removal of phenols and nitrophenols from aquatic systems, J. Appl. Polym. Sci., 83 (2002) 2411–2418.

[29] M. Ahmaruzzaman, D.K. Sharma, Adsorption of phenols from wastewater, J. Colloid Interface Sci., 287 (2005) 14–24.

[30] V.K. Gupta, I. Ali, V.K. Saini, Removal of chlorophenols from wastewater using red mud: an aluminum industry waste, Environ. Sci. Technol., 38 (2004) 4012–4018.

[31] V.C. Srivastava, M.M. Swamy, I.D. Mall, B. Prasad, I.M. Mishra, Adsorptive removal of phenol by bagasse fly ash and activated carbon: equilibrium, kinetics and thermodynamics, Colloids Surf., A, 272 (2006) 89–104.

[32] A.K. Jain, V.K. Gupta, S. Jain, S. Has, Removal of chlorophenols using industrial wastes, Environ. Sci. Technol., 38 (2004) 1195–1200.

[33] M. Otero, F. Rozada, L.F. Calvo, A.I. Garcıa, A. Moran, Elimination of organic water pollutants using adsorbents obtained from sewage sludge, Dyes Pigm., 57 (2003) 55–65.

[34] A.H. Sulaymon, K.W. Ahmed, Competitive adsorption of furfural and phenolic compounds onto activated carbon in fixed bed column, Environ. Sci. Technol., 42 (2008) 392–397.

[35] P.S. Nayak, B.K. Singh, Removal of phenol from aqueous solutions by sorption on low cost clay, Desalination, 207 (2007) 71–79.

[36] M.F. Elkady, H.S. Hassan, W.A. Amer, E. Salama, H. Algarni, E.R. Shaaban, Novel magnetic zinc oxide nanotubes for phenol adsorption: mechanism modeling, Materials, 10 (2017) 1355.

[37] M. Malakootian, H.J. Mansooriana, M. Alizadehd, A. Baghbaniane, Phenol removal from aqueous solution by adsorption process: study of the nanoparticles performance prepared from aloe vera and mesquite (prosopis) leaves, Sci. Iran., C24 (2017) 3041–3052.

[38] S. Lagergren, About the theory of so-called adsorption of soluble substances, K. Sven. Vetensk.akad. Handl., 24 (1898) 1–39.

[39] Y.S. Ho, G. McKay, Pseudo second order model for sorption processes, Process Biochem., 34 (1999) 451–465.

Supplementary figures

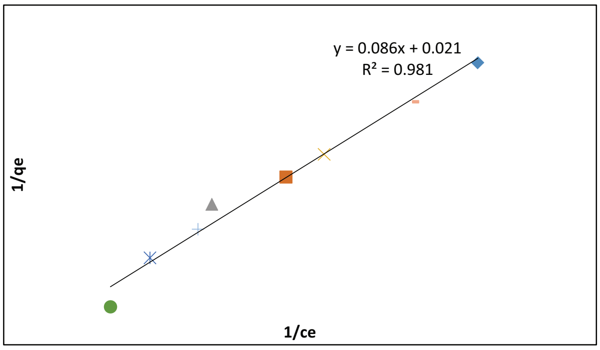

Fig. S1. Langmuir isotherm plots for the sorption of nZVI nanoparticles.

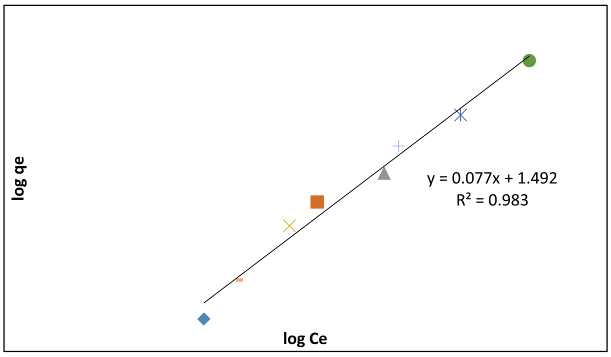

Fig. S2. Freundlich isotherm plots for the sorption of nZVI nanoparticles.

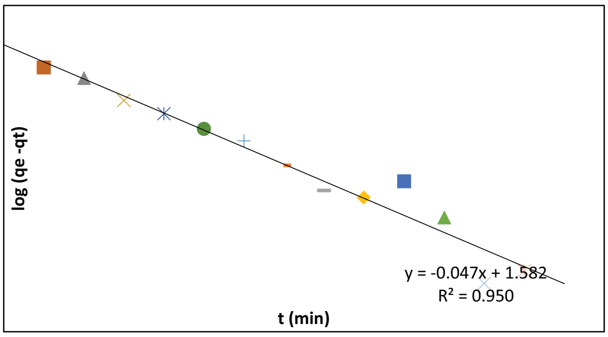

Fig. S3. Pseudo-first order plots for the sorption of nZVI nanoparticles.

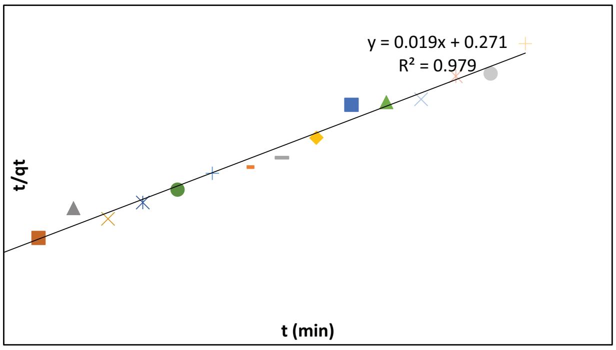

Fig. S4. Pseudo-second order plots for the sorption of nZVI nanoparticles.